Breast Cancer Res Treat (2013) 141:67–78
DOI 10.1007/s10549-013-2668-x

PRECLINICAL STUDY

Effects of sorafenib on energy metabolism in breast cancer cells: role of AMPK–mTORC1 signaling

Claudia Fumarola · Cristina Caffarra · Silvia La Monica · Maricla Galetti · Roberta R. Alfieri · Andrea Cavazzoni · Elena Galvani · Daniele Generali · Pier Giorgio Petronini · Mara A. Bonelli

Received: 5 March 2013 / Accepted: 9 August 2013 / Published online: 21 August 2013

Abstract In this study, we investigated the effects and the underlying molecular mechanisms of the multi-kinase inhibitor sorafenib in a panel of breast cancer cell lines. Sorafenib inhibited cell proliferation and induced apoptosis through the mitochondrial pathway. These effects were neither correlated with modulation of MAPK and AKT pathways nor dependent on the ERα status. Sorafenib promoted an early perturbation of mitochondrial function, inducing a deep depolarization of mitochondrial membrane, associated with drop of intracellular ATP levels and increase of ROS generation. As a response to this stress condition, the energy sensor AMPK was rapidly activated in all the cell lines analyzed. In MCF-7 and SKBR3 cells, AMPK enhanced glucose uptake by up-regulating the expression of GLUT-1 glucose transporter, as also demonstrated by AMPKα1 RNA interference, and stimulated aerobic glycolysis thus increasing lactate production. Moreover, the GLUT-1 inhibitor fasentin blocked sorafenib-induced glucose uptake and potentiated its cytotoxic activity in SKBR3 cells. Persistent activation of AMPK by sorafenib finally led to the impairment of glucose metabolism both in MCF-7 and SKBR3 cells as well as in the highly glycolytic MDA-MB-231 cells, resulting in cell death. This previously unrecognized long-term effect of sorafenib was mediated by AMPK-dependent inhibition of the mTORC1 pathway. Suppression of mTORC1 activity was sufficient for sorafenib to hinder glucose utilization in breast cancer cells, as demonstrated by the observation that the mTORC1 inhibitor rapamycin induced a comparable down-regulation of GLUT-1 expression and glucose uptake. The key role of AMPK-dependent inhibition of mTORC1 in sorafenib mechanisms of action was confirmed by AMPKα1 silencing, which restored mTORC1 activity conferring a significant protection from cell death. This study provides insights into the molecular mechanisms driving sorafenib anti-tumoral activity in breast cancer, and supports the need for going on with clinical trials aimed at proving the efficacy of sorafenib for breast cancer treatment.

Keywords Sorafenib · Breast cancer · mTORC1 · AMPK · Energy metabolism

C. Fumarola (✉) · C. Caffarra · S. La Monica · M. Galetti · R. R. Alfieri · A. Cavazzoni · E. Galvani · P. G. Petronini · M. A. Bonelli
Department of Clinical and Experimental Medicine, University of Parma, Via Volturno, 39, Parma 43125, Italy
e-mail: claudia.fumarola@unipr.it

D. Generali
Unità di Patologia Mammaria-Breast Cancer Unit, Istituti Ospitalieri di Cremona, Cremona, Italy

D. Generali
Centro di Medicina Molecolare, Istituti Ospitalieri di Cremona, Cremona, Italy

Introduction

The bisarylurea sorafenib (Nexavar, BAY43-9006) is a multi-kinase inhibitor with anti-proliferative and anti-angiogenic activity, approved for the treatment of unresectable hepatocellular carcinoma (HCC), and metastatic renal cell carcinoma [1, 2].

Sorafenib was initially identified as a potent inhibitor of Raf kinase isoforms (A-Raf, wild-type or mutated B-RafV600E, and C-Raf). However, it has been demonstrated that sorafenib as well as other Raf inhibitors can either suppress or activate the downstream signaling pathway depending on the presence of Raf or Ras

mutations [3, 4]. In addition, sorafenib potently inhibits the pro-angiogenic VEGFR, PDGFR-β, and other tyrosine kinase receptors such as c-Kit and Flt-3 [5, 6]. Sorafenib anti-proliferative action may also be associated with inhibition of mammalian target of rapamycin complex 1 (mTORC1) signaling, as our and other groups have previously shown in ERα-positive breast cancer (BC) and HCC cell lines [7, 8]. In addition, sorafenib induced apoptosis in several tumor cell lines, through down-regulation of the anti-apoptotic myeloid cell leukemia-1 protein (Mcl-1) and consequent activation of the mitochondrial pathway [9, 10], associated with mitochondrial membrane depolarization (MMD). MMD was merely seen as an initial event of mitochondria-dependent cell death processes, leading to the release of pro-apoptotic molecules, such as cytochrome *c* or AIF. However, emerging evidence suggests that sorafenib may have a more specific effect on mitochondria; indeed, it has been shown to inhibit oxidative phosphorylation (OXPHOS) in HCC [11] and to directly target mitochondrial electron transport chain complex I in neuroblastoma cells, impairing mitochondrial energy production [12].

Sorafenib is currently under evaluation in a variety of solid tumors and phase II/III clinical trials are ongoing in advanced/metastatic BC in combination with conventional chemotherapy or endocrine therapy. Recent results demonstrated a significant progression-free survival (PFS) benefit with the addition of sorafenib to first- or second-line capecitabine in metastatic HER2-negative BC [13]. A significant PFS benefit was also obtained by combining sorafenib with gemcitabine or capecitabine [14]. Recently, addition of sorafenib to paclitaxel was shown to improve disease control, although without significantly increasing PFS [15]. Finally, addition of sorafenib to anastrozole was associated with an increase in clinical benefit rate [16].

Despite the increasing number of clinical trials with sorafenib in BC, little is known about the molecular mechanisms underlying its anti-tumor activity. The present study was designed to investigate this aspect in a panel of BC cell lines of different subtypes, with particular attention on the effects on intracellular signaling pathways that control either cell proliferation/survival or energy metabolism.

Materials and methods

Cell culture

Human BC cell lines MCF-7, T47D, BT474 (ERα-positive), MDA-MB-231, MDA-MB-468 (triple negative), and SKBR3 (ERα-negative/HER2-positive), obtained from ATCC, were cultured in RMPI-1640 containing 10 % FBS, 1 % penicillin/streptomycin solution.

Chemicals and reagents

Sorafenib (Bayer HealthCare LLC, Tarrytown, NY), diphenyleneiodonium chloride (DPI, Merck Millipore), NVP-BEZ235 (Novartis Institutes for BioMedical Research, Basel, Switzerland), rapamycin, U0126, oligomycin (Sigma-Aldrich), and z-VAD-fmk (MP) were prepared in DMSO. DMSO concentration never exceeded 0.1 % (v/v) and equal amounts of DMSO were added to control cells. *N*-Acetyl-L-cysteine (NAC, Sigma-Aldrich) was directly dissolved into the medium before the experiments. 2-Deoxy-glucose (2DG, Sigma-Aldrich) was dissolved in bi-distilled water. Fasentin (Merck Millipore) was dissolved in 50 % DMSO in water.

Media and FBS were from Euroclone. Antibodies against phospho-ERK1/2 (Thr202/Tyr204), ERK1/2, phospho-AKT (Ser473), AKT, phospho-mTOR (Ser2448), mTOR, phospho-4E-BP1 (Ser65), phospho-p70S6K (Thr389), p70S6K, PARP-1, caspase-7, caspase-9, p-src, p-STAT3, Mcl-1, and p-AMPKα1 (Thr172) were from CST. Anti-GLUT-1 and anti-AMPKα1 antibodies were from Abcam. Anti-actin antibody was from Sigma-Aldrich. Horseradish peroxidase-conjugated secondary antibodies and the enhanced chemiluminescence system were from Millipore. Reagents for electrophoresis and blotting analysis were from Bio-Rad.

Western blotting

Procedures for protein extraction and analysis by 1D PAGE are described elsewhere [17]. For GLUT-1 detection, cells were lysed in GLUT-1 lysis buffer (1 % Triton X-100, 0.1 % SDS, protease inhibitors) for 1 h on ice, and precleared by centrifugation for 10 min at 4 °C. Protein extracts were denatured in sample buffer for 30 min before electrophoresis.

Analysis of cell proliferation and death

Cell proliferation/survival was evaluated by crystal-violet staining as previously described [17]. Cell death was assessed by fluorescence-microscopy after Hoechst-33342/propidium-iodide (PI) staining as previously described [18].

ATP, MMD, and reactive oxygen species (ROS) measurements

Cellular ATP changes were determined by a luminescence assay (ATPLite-1step, PerkinElmer).

MMD was measured as reduced staining with the potentiometric fluorescent dye tetramethylrhodamine–methylester (TMRM, Molecular Probes®). Intracellular hydrogen

peroxide H_2O_2 and superoxide anion O_2^- were assessed by oxidation of the cell permeable fluorescent probes 5-(and-6)-chloromethyl-2′,7′-dichlorodihydrofluorescein diacetate, acetyl ester (CM-H2DCFDA, Molecular Probes®), and dihydroethidium (DHE, Merck Millipore), respectively. 3×10^5 cells, seeded into 6-well plates, were incubated in different conditions depending on the experiment. During the last 30 min of treatment, the cells, loaded with TMRM 0.01 μM, CM-H2DCFDA 0.2 μM, or DHE 5 μM, were left in the dark at 37 °C, and then trypsinized and analyzed on a Beckman-Coulter EPICS XL flow cytometer.

Glucose uptake

Cells were grown to ~70 % confluence into 12-well plates and then subjected to different treatments. After 6–24 h, depending on the experiments, cells were rinsed with Kreb's Ringer HEPES buffer (KRH) and incubated in KRH containing 2 μCi/ml Deoxy-D-glucose-2-[1,2-^{3}H(N)] (PerkinElmer) at 37 °C for 5 min. Then, the cells were quickly rinsed three times in fresh cold Earle's solution containing 0.1 mM phloretin (Sigma-Aldrich). Ice-cold trichloroacetic acid (TCA, 5 %) was added and radioactivity in the acid extracts was measured by liquid-scintillation in four independent determinations. Cell proteins, precipitated by TCA, were dissolved in 0.5 N NaOH and their concentration determined by a dye-fixation method (Bio-Rad). Glucose uptake was calculated as pmol of Deoxy-D-glucose-2-[1,2-^{3}H(N)]/mg protein/5 min.

Glycolytic flux

Glytolytic flux was measured as described by Zhao et al. [19]. Cells were incubated as indicated for glucose uptake. After 6–24 h, they were washed in PBS, pre-incubated in drug-containing or drug-free KRH buffer for 30 min, and then incubated with 10 μCi/ml D-glucose[5-^{3}H(N)] (PerkinElmer) and unlabeled D-glucose (10 mM final concentration). After 1 h at 37 °C, the reaction was stopped by adding HCl (0.04 M final concentration). ^3H_2O was separated from [5-^{3}H]glucose by diffusion in an airtight container for 72 h. Radioactivity was measured by liquid-scintillation. Cell proteins, precipitated by HCl, were dissolved in 0.5 N NaOH and their concentration determined by a dye-fixation method. Glucose utilization rates were calculated as described by Ashcroft et al. [20].

Lactate production

Cells were incubated as indicated for glucose uptake. After 6 h, media were collected and lactate was measured in accordance with the manufacture's instructions by a colorimetric assay kit (Biochemical Enterprise).

RNA interference assay

Cells were transfected with siRNA against AMPKα1 (Ambion Silencer® Select siRNA 4392420, mixture of s100, s101, s102 antisense sequences) or Silencer® Select negative control siRNA with a final concentration of 60 nM.

The transfection was carried out according to the Invitrogen reverse transfection protocol for Lipofectamine™ RNAiMAX transfection reagent. After 48 h, the medium was replaced with fresh medium for subsequent analysis.

Statistical analysis

Statistical significance of differences among data was estimated by two-tailed Student's t test. Differences were considered significant at $p < 0.05$ ($^*p < 0.05$; $^{**}p < 0.01$; $^{***}p < 0.001$).

IC_{50} values, expressed as mean ± SD of three independent determinations, were calculated by fitting the experimental data with a hyperbolic function and constraining Y_{max} to 100. Data were analyzed using GraphPad Prism 4.00 software.

Results

Sorafenib differently affects cell proliferation/survival and growth signaling pathways in BC cell lines

The effects of sorafenib were evaluated in a panel of BC cell lines of different subtypes. Sorafenib inhibited cell proliferation with IC_{50} values ranging from 2.1 to 5.9 μM (Fig. 1a). As shown in Fig. 1b, c, phospho-ERK1/2 and phospho-AKT levels decreased in the ERα-negative MDA-MB-231 and SKBR3 cells, and increased or remained unchanged in the ERα-positive cell models as well as in MDA-MB-468 ERα-negative cells, suggesting that sorafenib-mediated effects are neither correlated with modulation of MAPK and AKT pathways nor dependent on the ERα status. In contrast, the phosphorylation of mTORC1 and its targets p70S6K and 4E-BP1 significantly decreased in all the cell lines (Fig. 1b, c), thus pointing to the inhibition of mTORC1 signaling as a general, central mechanism of sorafenib action in BC. Sorafenib at 5–7.5 μM induced cell death in all the cell lines although to different extents (Fig. 2a). Cell death occurred through the apoptotic intrinsic pathway, as indicated by cleavage of the caspase substrate PARP-1 and activation of caspase-9 and caspase-7 (Fig. 2b). In addition, the anti-apoptotic protein Mcl-1 was down-regulated, presumably as a consequence of STAT3 inhibition (Fig. 2c). Sorafenib was shown to suppress STAT3 phosphorylation by inhibiting

src-kinase activity in leukemic cells [21]. However, p-src down-regulation occurred in MCF-7 and SKBR3, but not in MDA-MB-231 cells, indicating that in this model a different mechanism is implicated in p-STAT3 inhibition (Fig. 2c). Treatment with the pan-caspase inhibitor z-VAD-fmk failed to inhibit cell death completely in SKBR3 cells, suggesting that caspase-independent pathways might also be involved in the cytotoxic action of sorafenib (Fig. 2d).

Sorafenib induces the activation of 5′-AMP-activated protein kinase (AMPK) as a consequence of mitochondrial ATP depletion

Based on previous findings demonstrating that sorafenib impaired mitochondrial energy production in rat myogenic and HCC cells [11, 22], we evaluated whether the emergence of an energy stress might have a role in the antitumoral activity of sorafenib in BC cells. First, we observed that a 2-h treatment with sorafenib induced the phosphorylation/activation of AMPK (Fig. 3a), a master energy stress sensor that, in response to increased cellular AMP:ATP ratio, switches on the catabolic pathways and switches off the anabolic pathways, in order to restore the energy balance. Actually, a significant drop of ATP intracellular levels was induced by a 2-h sorafenib treatment in MCF-7, MDA-MB-231, and SKBR3 cells (Fig. 3b). These cell lines were selected for the subsequent experiments as models representative of each BC subtype and showing different metabolic behavior. Preliminary results (not shown) and data from literature indicate that MCF-7 cells are mainly dependent on mitochondrial respiration, the more aggressive MDA-MB-231 cells display a glycolytic phenotype, whereas SKBR3 cells have an intermediate bioenergetic organization. MCF-7, MDA-MB-231, and SKBR3 cells were incubated with sorafenib, oligomycin (a mitochondrial ATPase inhibitor), and 2DG (a non-metabolizable glucose analog that blocks glycolysis) alone or in combination. As shown in Fig. 4a, MCF-7 cells were the most sensitive to either sorafenib- or oligomycin-mediated effects on ATP levels. When sorafenib and oligomycin were used in combination, intracellular ATP decreased to levels comparable to those observed with each agent alone, both in MCF-7 cells as well as in MDA-MB-231 and SKBR3 cells. In contrast, ATP levels were further lowered by the combination of sorafenib with 2DG as compared with single agents, mimicking the effect of oligomycin-2DG combination. These data suggest that sorafenib, as oligomycin, led to ATP decrease and energy stress by affecting mitochondrial respiration in BC cell lines, confirmed also by the observation that sorafenib induced a MMD (Fig. 4b), associated with an increase of ROS

a

Cell line	Sorafenib IC_{50} (μM)
MCF-7	2.9 ± 0.3
T47D	2.1 ± 0.1
BT474	2.3 ± 0.2
MDA-MB-231	5.9 ± 0.1
MDA-MB-468	5.0 ± 0.5
SKBR3	3.2 ± 0.4

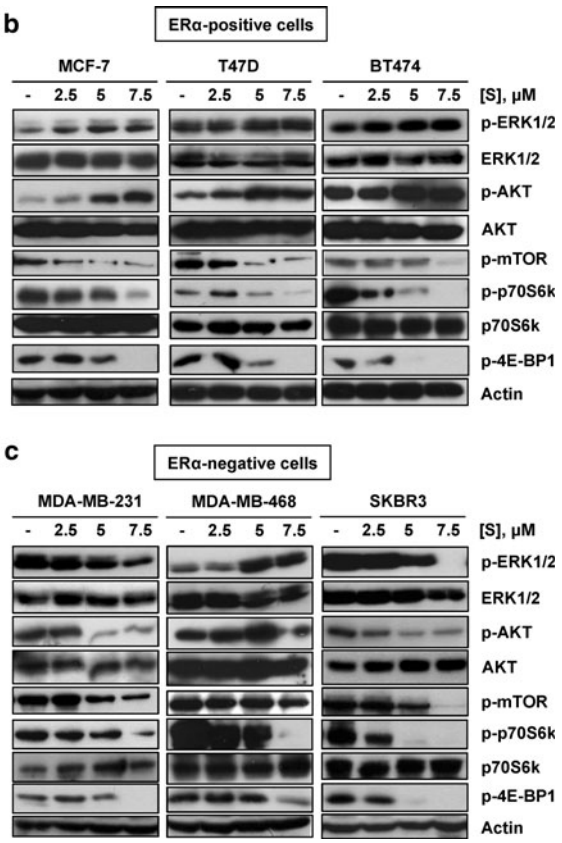

Fig. 1 Effects of sorafenib on cell proliferation and growth signaling pathways. **a** 3–5 × 10^3 cells, seeded in 96-multiwell plates, were treated with or without increasing concentrations of sorafenib (0.1–10 μM). After 72 h, cell proliferation was assessed using crystal-violet staining. IC_{50} values ± SD are shown. ERα-positive (**b**) and ERα-negative (**c**) BC cells were treated with or without various concentrations of sorafenib (*S*). After 24 h, expression of the indicated proteins was analyzed by western blotting. Results are representative of three independent experiments

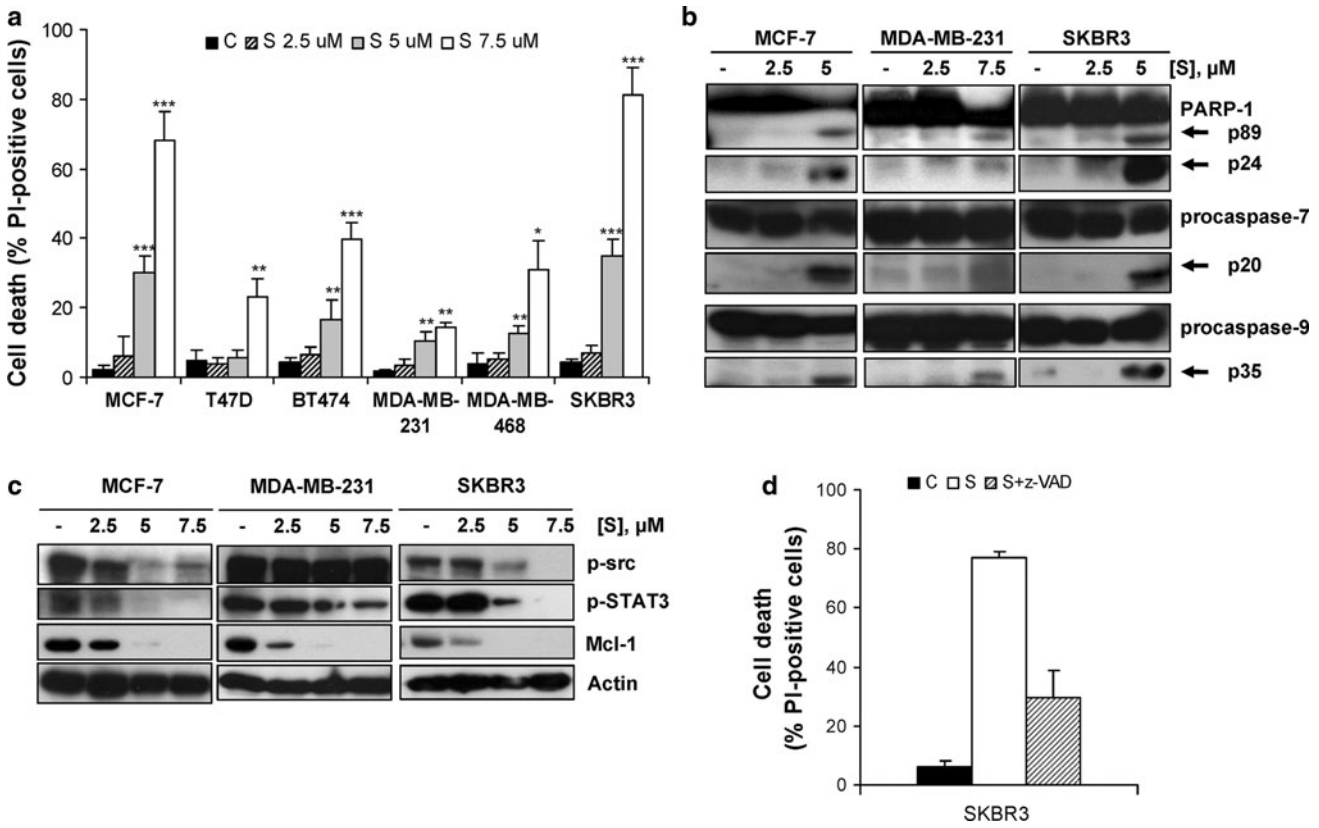

Fig. 2 Effects of sorafenib on cell survival. Cells were treated in the absence (*C*) or presence of the indicated concentrations of sorafenib (*S*). **a** Cell death was quantitated after 72 h on Hoechst 33342/PI-stained cells. *Columns* mean of three independent experiments; *bars* SD. **b** PARP-1, procaspase-7, and procaspase-9 cleavage were assessed by western blotting after 72 h. **c** p-src, p-STAT3, Mcl-1, and Actin protein expression were evaluated by western blotting after 48 h. Results in **b**, and **c** are representative of three independent experiments. **d** SKBR3 cells were untreated (*C*) or treated with sorafenib 7.5 μM in the absence (*S*) or presence of the pan-caspase inhibitor z-VAD-fmk 50 μM (*S* + z-VAD). After 72 h, cell death was quantitated as described in a. *Columns* mean of three independent experiments, *bars* SD

generation up to 24 h (Fig. 4c). Both effects were evident as early as 1 h after sorafenib exposure, when also AMPK appeared significantly induced (Fig. 4d). It is noteworthy that accumulation of ROS might contribute to AMPK activation that persisted during prolonged incubations with sorafenib (Fig. 4d). To get insight into the role of ROS generation in the mechanisms of sorafenib action, MCF-7 cells were incubated with NAC, a precursor of reduced glutathione (GSH) which acts as a H_2O_2 scavenger. Despite reducing sorafenib-mediated production of H_2O_2 (Fig. 4e), NAC failed to protect the cells from death (Fig. 4f). As shown in Fig. 4e, sorafenib increased also the production of O_2^-, on which NAC had no relevant effect. Based on a previous study demonstrating the role of NADPH oxidase-dependent production of O_2^- in sorafenib effectiveness in HCC [23], we pre-treated MCF-7 cells with the NADPH oxidase inhibitor DPI before exposure to sorafenib. However, DPI promoted instead of inhibiting ROS production, and further enhanced both H_2O_2 and O_2^- induced by sorafenib (Fig. 4e). In accordance, DPI potentiated the cytotoxic action of sorafenib (Fig. 4f).

Sorafenib produces opposite early and long-term effects on glucose metabolism

We evaluated whether sorafenib-mediated impairment of oxidative phosphorylation affected cell glucose metabolism. In MCF-7 and SKBR3 cells, a 6-h treatment with sorafenib increased glucose uptake (Fig. 5a) by up-regulating the expression of GLUT-1 glucose transporter (Fig. 5b), stimulated aerobic glycolysis (Fig. 5c) to compensate for the loss of mitochondrial ATP, and increased lactate production (Fig. 5d). After 24 h of treatment these effects were still maintained in SKBR3 cells, whereas in MCF-7 cells either glucose transport or consumption were decreased (Fig. 5a–c). However, a more prolonged exposure to sorafenib ultimately hindered glucose utilization also in SKBR3 cells, as suggested by inhibition of GLUT-1 expression after 48 h of treatment (Fig. 5b). In the highly glycolytic MDA-MB-231 cells, sorafenib-induced mitochondrial perturbation slightly affected glucose metabolism after 6 h (Fig. 5a–d); however, a significant down-regulation of GLUT-1 expression, glucose transport, and

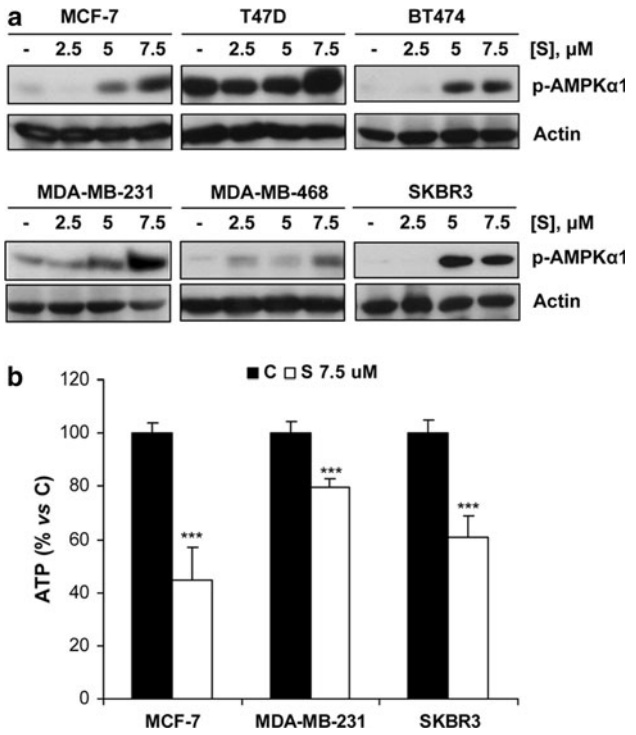

Fig. 3 Sorafenib early induces AMPK activation and ATP depletion. **a** Cells were incubated in the absence or presence of sorafenib (*S*) at the indicated concentrations. p-AMPKα1 expression was analyzed after 2 h by western blotting. Results are representative of three independent experiments. **b** Cells were incubated in the absence (*C*) or presence of sorafenib (*S* 7.5 μM). After 2 h, ATP levels were measured by a luminescence assay. *Columns* mean of three independent experiments, *bars* SD

glycolysis was observed after 24 h and persisted after 48 h, as suggested by inhibition of GLUT-1 expression. Interestingly, incubation of SKBR3 cells with the GLUT-1 inhibitor fasentin down-regulated the basal uptake of glucose and inhibited the uptake induced by sorafenib (Fig. 5e), indicating that GLUT-1 is the glucose transporter actually involved in sorafenib-mediated effects on glucose metabolism. In addition, fasentin, by inhibiting glucose utilization, rendered SKBR3 cells unable to compensate for sorafenib-induced impairment of OXPHOS, thus potentiating sorafenib cytotoxic action (Fig. 5f). All together these results indicate that, despite the initial attempt to adapt to the energy stress through AMPK activation and GLUT-1 induction, BC cells exposed to sorafenib ultimately experienced a significant impairment of glucose metabolism, which might contribute to sorafenib cytotoxic activity.

Sorafenib-mediated down-regulation of glucose metabolism involves inhibition of mTORC1 signaling

Although AMPK might be responsible for the enhancement of glycolysis at early time points after sorafenib exposure, its persistent activation may produce the opposite effect on glucose metabolism through down-regulation of mTORC1 signaling. To evaluate whether this mechanism could be sufficient to hamper glucose utilization during sorafenib treatment, MCF-7 cells were treated for 24 h with sorafenib, the mTORC1 inhibitor rapamycin, the dual PI3K/mTORC1-C2 inhibitor NVP-BEZ-235, or the MEK1/2 inhibitor U0126. As indicated in Fig. 6a, b, U0126 had no effect, while rapamycin and sorafenib down-regulated both GLUT-1 expression and glucose uptake to similar extents. A deeper effect was produced by NVP-BEZ-235, due to the simultaneous inhibition of AKT and mTORC1. These results suggest that sorafenib-mediated inhibition of mTORC1 signaling, possibly consequent to persistent AMPK activation, was sufficient to alter glucose metabolism in BC cells.

AMPKα1 silencing has a significant impact on sorafenib-mediated effects

To clearly demonstrate the role of AMPK activation in the early effects mediated by sorafenib and to further validate the relevance of AMPK-dependent inhibition of mTORC1 in sorafenib long-term action, we down-regulated AMPKα1 expression by RNA interference. As shown in Fig. 7a, b AMPKα1 silencing did not prevent sorafenib-mediated induction of MMD and ROS production, implying that both these events preceded AMPK activation. In addition, AMPKα1 knockdown blocked the increase of GLUT-1 protein expression induced by a 6-h treatment with sorafenib (Fig. 7c), and prevented the down-regulation of mTORC1 signaling observed after 24 h (Fig. 7d). These results indicate that AMPK activation is required to stimulate glucose metabolism as an early adaptation to sorafenib-mediated energy stress and definitely demonstrate that long-term exposure to sorafenib inhibits the mTORC1 pathway through an AMPK-dependent mechanism in BC cells. Importantly, restoration of mTORC1 signaling by AMPKα1 silencing reduced the cytotoxic effects of sorafenib (Fig. 7e).

Discussion

In the present study we provide evidence that sorafenib anti-tumor activity in BC cells is mediated by a Raf/MEK/ERK-independent, AMPK/mTORC1-dependent mechanism that involves the induction of energy stress.

Data from our and other groups on the effects of sorafenib in BC in vitro, mainly in combination with other drugs, are already available [7, 10, 24–26]. However, to our knowledge, a comprehensive study aimed at defining the molecular mechanisms of sorafenib action through comparison of BC cell lines of different subtypes had been

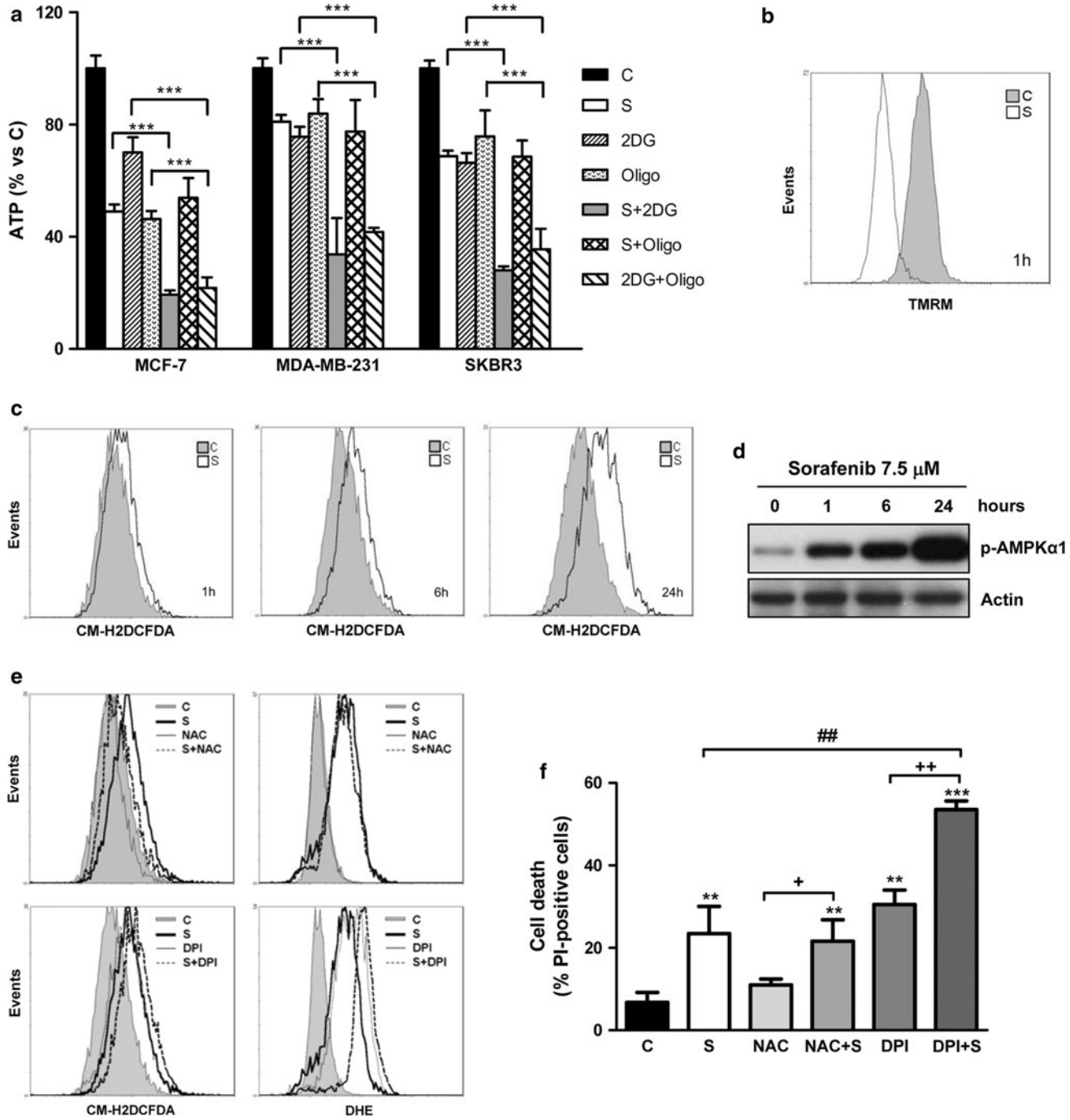

Fig. 4 Sorafenib impairs mitochondrial function, causing MMD and increasing ROS production. **a** Cells were untreated (*C*) or treated with sorafenib 7.5 μM (*S*), 2DG 10 mM, and oligomycin 20 μg/ml (Oligo) either alone or in combination ($S + 2DG$, $S + Oligo$, $2DG + Oligo$). After 2 h, ATP levels were measured by a luminescence assay. *Columns* mean of three independent experiments, *bars* SD. MCF-7 cells were incubated in the absence (*C*) or presence of sorafenib 7.5 μM (*S*). MMD (**b**), ROS (more specifically H_2O_2) (**c**), p-AMPKα1 and Actin expression (**d**) were analyzed at the time points indicated. Results are representative of three independent experiments. MCF-7 cells were incubated in the absence (*C*) or presence of sorafenib 7.5 μM (*S*), NAC 5 mM, DPI 10 μM either alone or in combination ($S + NAC$, $S + DPI$). After 6 h, production of H_2O_2 and O_2^- was measured by using CM-H2DCFDA and DHE probes, respectively (**e**). Results are representative of three independent experiments. After 24 h, cell death was quantitated on Hoechst 33342/PI-stained cells (**f**). *Columns* mean of three independent experiments, *bars* SD. *Statistical significance versus *C*

never performed. Here we show that sorafenib-mediated inhibition of cell proliferation was associated with down-regulation of mTORC1 signaling in all the cell lines selected. In a previous study, sorafenib was shown to inhibit the MAPK pathway in MDA-MB-231 cells containing activating mutations in both K-Ras and B-Raf

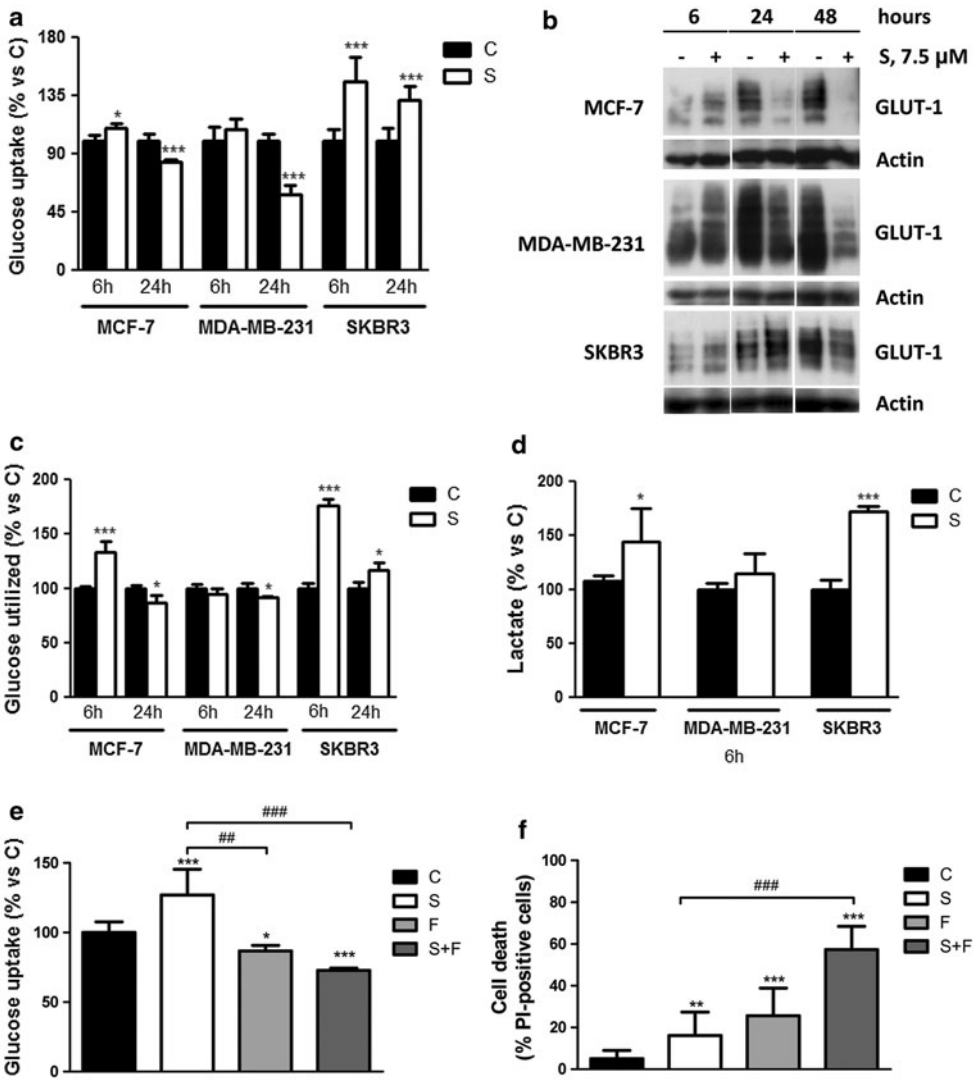

Fig. 5 Sorafenib affects glucose metabolism. Cells were incubated in the absence (*C*) or presence of sorafenib 7.5 μM (*S*). Glucose uptake (**a**), GLUT-1 and Actin protein expression (**b**), glycolysis (**c**), and lactate production (**d**) were analyzed at the time points indicated. SKBR3 cells were untreated (*C*) or treated with sorafenib 7.5 μM (*S*) and fasentin 200 μM (*F*) either alone or in combination (*S* + *F*). Glucose uptake (**e**) and cell death on Hoechst 33342/PI-stained cells (**f**) were analyzed after 6 and 24 h, respectively. *Columns* in **a**, **c**–**f** mean of three independent experiments, *bars* SD. *Statistical significance versus *C*. Results in **b** are representative of three independent experiments

proto-oncogenes, suggesting this as a general mechanism for sorafenib activity in BC [5, 27].

Based on our results, MAPK inhibition could effectively contribute to the growth-inhibitory effects of sorafenib in MDA-MB-231 cells and in SKBR3 cells. However, this conclusion cannot be generalized, since ERK1/2 phosphorylation/activation increased upon sorafenib treatment in the other cell models, presumably due to Ras-dependent C-Raf homo/heterodimerization and activation [3] or to the release of mTOR-dependent feedback inhibition of RTK/IRS-1/Ras/MAPK signaling [28].

By relieving the negative feedback on IRS-1, sorafenib-mediated down-regulation of mTORC1 signaling may be also responsible for the phosphorylation/activation of AKT observed in MCF-7, T47D, and BT474 ERα-positive cells as well as in MDA-MB-468 triple negative cells. This phenomenon may be explained considering that these cells are characterized by an aberrant activation of the PI3K signaling pathway, due to PIK3CA mutations in the ERα-positive cell lines and to PTEN mutations in MDA-MB-468 cells. Indeed, a recent study on cancer cell sensitivity to mTOR inhibitors demonstrated that rapamycin-mediated activation of AKT signaling is greater in rapamycin sensitive cells and that these cells are more likely to have PIK3CA and/or PTEN mutations [29]. Taken together, our results suggest that the observed differences in sorafenib-mediated effects on MAPK and AKT signaling are correlated with genetic features other than the ERα status that defines BC standard classification.

Sorafenib at 5–7.5 μM induced apoptosis through the intrinsic pathway, although activation of caspase-independent pathways cannot be ruled out. It is noteworthy that MDA-MB-231 cells appeared less prone to undergo apoptosis as compared with the other cell lines, showing a significant lower percentage of cell death after 72 h of treatment. This result reinforces the suggestion that inhibition of MAPK pathway cannot be considered as a predictive factor of sorafenib sensitivity in BC. These data

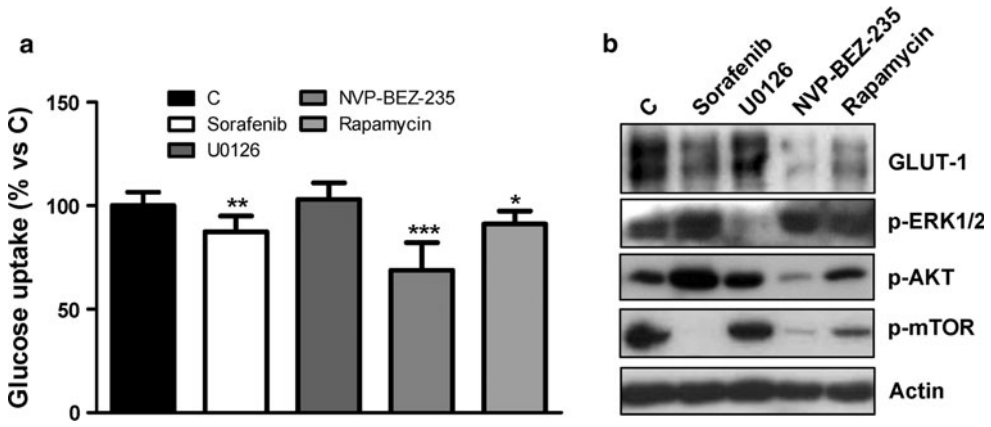

Fig. 6 Inhibitors of proliferation/survival signaling pathways differently affect glucose utilization in MCF-7 cells. MCF-7 cells were incubated in the absence (*C*) or presence of sorafenib 7.5 μM, U0126 3 μM, NVP-BEZ-235 0.1 μM, or Rapamycin 0.1 μM. Glucose uptake (**a**) and western blotting (**b**) were performed after 24 h. *Columns* in **a** mean of two independent experiments, *bars* SD. Results in **b** are representative of two independent experiments

agree with previous works delineating different MAPK-independent mechanisms to explain sorafenib action in a variety of cancer cell types [30–33]. It is becoming clear that sorafenib acts through mechanisms that involve multiple targets, including novel unexpected molecules [34]. Among these, the mitochondrial electron transport chain complex I has been recently identified in neuroblastoma cells as an early sorafenib's target, whose down-regulation, through protein destabilization, causes a rapid caspase-independent MMD [12]. Inhibition of complex I enzyme activity may account for both MMD and impairment of OXPHOS that we observed in BC cells as early effects of sorafenib treatment. As a consequence of these events, ATP levels decreased in all the cell lines analyzed, although this reduction was more pronounced in MCF-7 cells, whose energy metabolism is mainly based on mitochondrial activity. ATP depletion, in turn, rapidly induced the phosphorylation/activation of the energy sensor AMPK. Upon activation, AMPK has been shown to stimulate glucose uptake, either by promoting the translocation of GLUTs to the plasma membrane, or by enhancing the transcription of genes encoding for these transporters [35]. In addition, AMPK may favor glycolysis by phosphorylating and activating 6-phosphofructo-2-kinase [36, 37]. Here we demonstrate that sorafenib-mediated activation of AMPK initially stimulated glucose uptake by increasing GLUT-1 protein expression in MCF-7 and SKBR3 cells. GLUT-1 induction was prevented by AMPKα1 silencing; moreover, the GLUT-1 inhibitor fasentin inhibited the glucose uptake induced by sorafenib, thus indicating that GLUT-1 is the glucose transporter actually involved in sorafenib-mediated effects on glucose metabolism. Sorafenib enhanced also glycolysis in MCF-7 and SKBR3 cells, consequently increasing lactate production. All these effects were observed after 6 h of sorafenib treatment. In contrast, no significant change in glucose metabolism was detected at this time point in MDA-MB-231 cells, which display a highly glycolytic phenotype and experienced a moderate decrease of ATP levels.

Although AMPK is considered essential for metabolic adaptation during energy stress conditions associated with suppression of OXPHOS, its activation has been shown to be transient [36, 38]. In contrast, we found that activation of AMPK persisted all along sorafenib treatment, suggesting that the energy stress could not be overcome despite the initial metabolic adjustments. It is noteworthy that a further contribution to maintenance of AMPK activation might derive from sorafenib-induced increase of ROS production, being AMPK also involved in the cell response to oxidative stress [39]. Intracellular ROS in BC cells increased early upon sorafenib exposure and further accumulated during the treatment. In a recent paper by Coriat et al. [23], sorafenib effectiveness in HCC was associated with NADPH oxidase-dependent production of O_2^-. In accordance with this study, we demonstrated that the H_2O_2 scavenger NAC, being unable to reduced O_2^- production, did not reduce the growth-inhibitory effects of sorafenib in MCF-7 cells. In contrast, the NADPH oxidase inhibitor DPI, that was shown to hinder both the generation of ROS and the induction of apoptosis in HCC cells, acted in the opposite manner in MCF-7 cells, increasing ROS and potentiating sorafenib activity. This result finds support in previous studies showing that DPI, instead of protecting, may augment oxidative stress and exert cytotoxic effects in some cellular systems [40].

Persistence of the energy stress during sorafenib treatment in BC cells resulted in a previously unrecognized inhibitory effect on glucose metabolism. Indeed, either GLUT-1 protein expression and hence glucose uptake or glycolysis were down-regulated after a prolonged exposure to the drug. We

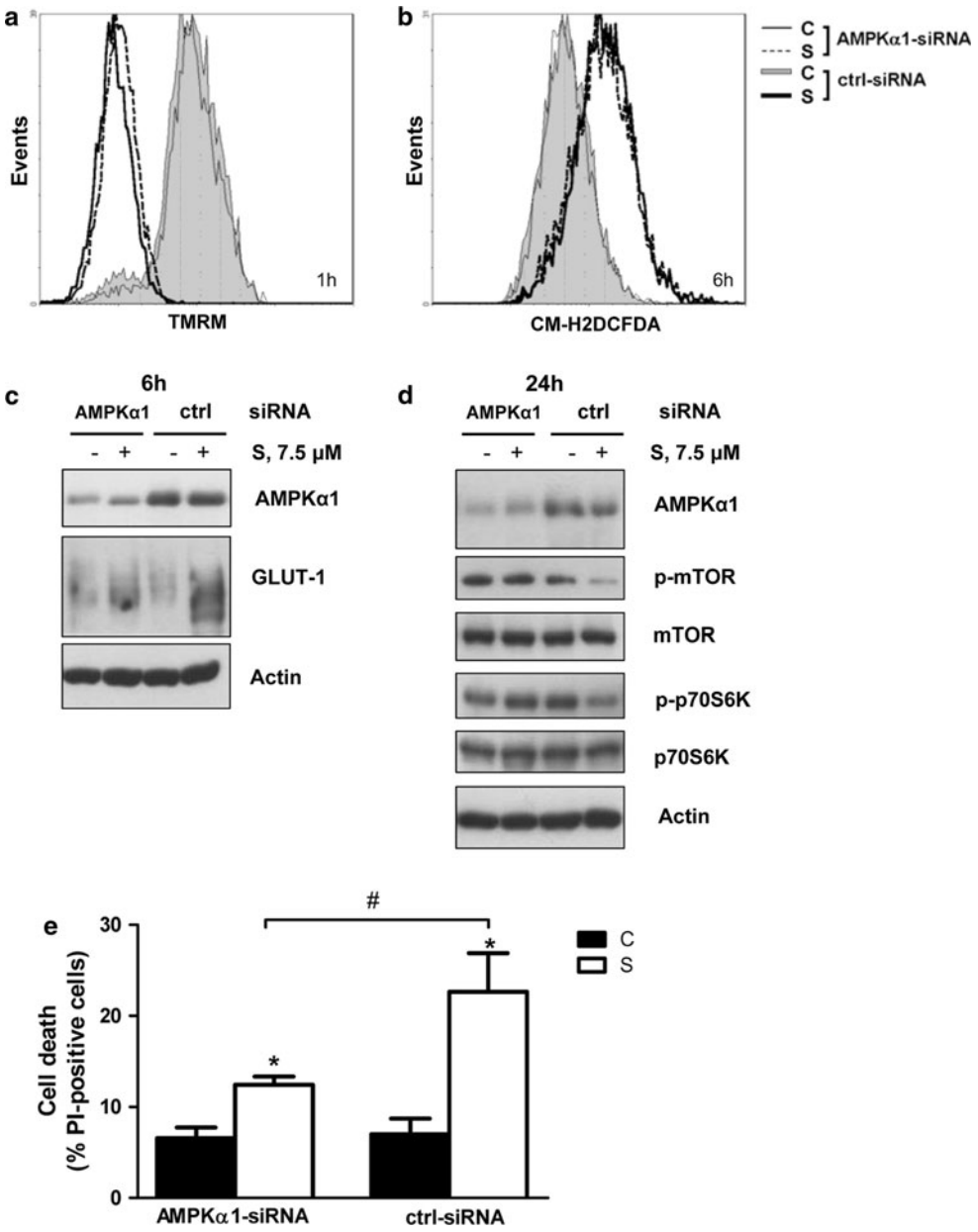

Fig. 7 AMPKα1 silencing alters sorafenib-mediated effects. MCF-7 cells were transfected with AMPKα1 or control siRNA. After 48 h, the medium was replaced with fresh medium with or without sorafenib 7.5 μM. At the time points indicated the following analyses were performed: MMD (**a**), H_2O_2 assessment (**b**), western blotting (**c**, **d**), cell death on Hoechst 33342/PI-stained cells (**e**). Results in **a**–**d** are representative of three independent experiments. *Columns* in **e** mean of three independent experiments, *bars* SD. *Statistical significance versus *C*

suggest that these long-term effects, despite being opposite to the acute stress response induced by AMPK, are still dependent on AMPK. Indeed, persistent activation of AMPK by sorafenib resulted in the inhibition of mTORC1 signaling, whose role in the regulation of glucose metabolism is well established [41]. mTORC1 is recognized as a master metabolic sensor that integrates nutrient and mitogen signals to regulate cell growth/division, by promoting protein synthesis and activating bioenergetic and anabolic processes, such as glycolysis. AMPK provides the link with the energy status of the cell, to allow proliferation only under conditions of sufficient energy supply. Therefore, AMPK activation by energy stress may lead to suppression of mTORC1 signaling even in the presence of growth factors and active AKT and ERK signaling [42]. Here we demonstrate that inhibition of mTORC1 is sufficient to hinder glucose utilization in BC cells, as indicated by the ability of the mTORC1 inhibitor rapamycin to down-regulate both GLUT-1 protein expression and glucose uptake in MCF-7 cells, effect enforced by NVP-BEZ-235, a dual PI3K/mTORC1-C2 inhibitor.

The importance of AMPK-dependent inhibition of mTORC1 in sorafenib mechanisms of action was clearly demonstrated by using AMPKα1 RNA interference; indeed, APMK depletion in MCF-7 cells restored mTORC1 activity at 24 h, conferring a significant protection from cell death.

Sorafenib, as also indicated by our study, has a broad spectrum of activity often independent of its canonical targets. Therefore, it is difficult to define a predictive

biomarker of sensitivity for this drug. In a recent work performed on HCC cell lines and xenografts, sorafenib resistance has been correlated with the bioenergetic propensity to use glycolysis [43]. However, caution should be used in extending this conclusion to BC cells. Indeed, the highly glycolytic MDA-MB-231 cells cannot be considered resistant to sorafenib, despite being less sensitive than other cell models that mainly rely on mitochondrial ATP production for their energy demands. Our results suggest that sorafenib, being effective in all the BC cell subtypes, may be proposed as a valid support to the current established therapy for ERα-positive or HER-positive BC. In triple negative BC subtype, its use in clinical practice warrants further validations.

Acknowledgments We thank Bayer HealthCare Pharmaceuticals for providing sorafenib and A.VO.PRO.RI.T., Parma, Italy for its support.

Conflict of interest The authors declare that they have no conflict of interest.

References

1. Kane RC, Farrell AT, Saber H, Tang S, Williams G, Jee JM, Liang C, Booth B, Chidambaram N, Morse D, Sridhara R, Garvey P, Justice R, Pazdur R (2006) Sorafenib for the treatment of advanced renal cell carcinoma. Clin Cancer Res 12(24):7271–7278
2. Kane RC, Farrell AT, Madabushi R, Booth B, Chattopadhyay S, Sridhara R, Justice R, Pazdur R (2009) Sorafenib for the treatment of unresectable hepatocellular carcinoma. Oncologist 14(1):95–100
3. Hatzivassiliou G, Song K, Yen I, Brandhuber BJ, Anderson DJ, Alvarado R, Ludlam MJ, Stokoe D, Gloor SL, Vigers G, Morales T, Aliagas I, Liu B, Sideris S, Hoeflich KP, Jaiswal BS, Seshagiri S, Koeppen H, Belvin M, Friedman LS, Malek S (2010) RAF inhibitors prime wild-type RAF to activate the MAPK pathway and enhance growth. Nature 464(7287):431–435
4. Poulikakos PI, Zhang C, Bollag G, Shokat KM, Rosen N (2010) RAF inhibitors transactivate RAF dimers and ERK signalling in cells with wild-type BRAF. Nature 464(7287):427–430
5. Wilhelm SM, Carter C, Tang L, Wilkie D, McNabola A, Rong H, Chen C, Zhang X, Vincent P, McHugh M, Cao Y, Shujath J, Gawlak S, Eveleigh D, Rowley B, Liu L, Adnane L, Lynch M, Auclair D, Taylor I, Gedrich R, Voznesensky A, Riedl B, Post LE, Bollag G, Trail PA (2004) BAY 43-9006 exhibits broad spectrum oral antitumor activity and targets the RAF/MEK/ERK pathway and receptor tyrosine kinases involved in tumor progression and angiogenesis. Cancer Res 64(19):7099–7109
6. Plaza-Menacho I, Mologni L, Sala E, Gambacorti-Passerini C, Magee AI, Links TP, Hofstra RM, Barford D, Isacke CM (2007) Sorafenib functions to potently suppress RET tyrosine kinase activity by direct enzymatic inhibition and promoting RET lysosomal degradation independent of proteasomal targeting. J Biol Chem 282(40):29230–29240
7. Bonelli MA, Fumarola C, Alfieri RR, La Monica S, Cavazzoni A, Galetti M, Gatti R, Belletti S, Harris AL, Fox SB, Evans DB, Dowsett M, Martin LA, Bottini A, Generali D, Petronini PG (2010) Synergistic activity of letrozole and sorafenib on breast cancer cells. Breast Cancer Res Treat 124(1):79–88
8. Huynh H, Ngo VC, Koong HN, Poon D, Choo SP, Thng CH, Chow P, Ong HS, Chung A, Soo KC (2009) Sorafenib and rapamycin induce growth suppression in mouse models of hepatocellular carcinoma. J Cell Mol Med 13(8B):2673–2683
9. Yu C, Bruzek LM, Meng XW, Gores GJ, Carter CA, Kaufmann SH, Adjei AA (2005) The role of Mcl-1 downregulation in the proapoptotic activity of the multikinase inhibitor BAY 43-9006. Oncogene 24(46):6861–6869
10. Ding Q, Huo L, Yang JY, Xia W, Wei Y, Liao Y, Chang CJ, Yang Y, Lai CC, Lee DF, Yen CJ, Chen YJ, Hsu JM, Kuo HP, Lin CY, Tsai FJ, Li LY, Tsai CH, Hung MC (2008) Down-regulation of myeloid cell leukemia-1 through inhibiting Erk/Pin 1 pathway by sorafenib facilitates chemosensitization in breast cancer. Cancer Res 68(15):6109–6117
11. Fiume L, Manerba M, Vettraino M, Di Stefano G (2011) Effect of sorafenib on the energy metabolism of hepatocellular carcinoma cells. Eur J Pharmacol 670(1):39–43
12. Bull VH, Rajalingam K, Thiede B (2012) Sorafenib-induced mitochondrial complex I inactivation and cell death in human neuroblastoma cells. J Proteome Res 11(3):1609–1620
13. Baselga J, Segalla JG, Roche H, Del Giglio A, Pinczowski H, Ciruelos EM, Filho SC, Gomez P, Van Eyll B, Bermejo B, Llombart A, Garicochea B, Duran MA, Hoff PM, Espie M, de Moraes AA, Ribeiro RA, Mathias C, Gil Gil M, Ojeda B, Morales J, Kwon Ro S, Li S, Costa F (2012) Sorafenib in combination with capecitabine: an oral regimen for patients with HER2-negative locally advanced or metastatic breast cancer. J Clin Oncol 30(13):1484–1491
14. Hudis C, Tauer KW, Hermann G, et al (2011) Sorafenib (SOR) plus chemotherapy (CRx) for patients (pts) with advanced (adv) breast cancer (BC) previously treated with bevacizumab (BEV). J Clin Oncol 29(suppl; abstr 1009)
15. Gradishar WJ, Kaklamani V, Sahoo TP, Lokanatha D, Raina V, Bondarde S, Jain M, Ro SK, Lokker NA, Schwartzberg L (2013) A double-blind, randomised, placebo-controlled, phase 2b study evaluating sorafenib in combination with paclitaxel as a first-line therapy in patients with HER2-negative advanced breast cancer. Eur J Cancer 49(2):312–322
16. Isaacs C, Herbolsheimer P, Liu MC, Wilkinson M, Ottaviano Y, Chung GG, Warren R, Eng-Wong J, Cohen P, Smith KL, Creswell K, Novielli A, Slack R (2011) Phase I/II study of sorafenib with anastrozole in patients with hormone receptor positive aromatase inhibitor resistant metastatic breast cancer. Breast Cancer Res Treat 125(1):137–143
17. La Monica S, Galetti M, Alfieri RR, Cavazzoni A, Ardizzoni A, Tiseo M, Capelletti M, Goldoni M, Tagliaferri S, Mutti A, Fumarola C, Bonelli M, Generali D, Petronini PG (2009) Everolimus restores gefitinib sensitivity in resistant non-small cell lung cancer cell lines. Biochem Pharmacol 78(5):460–468
18. Fumarola C, La Monica S, Alfieri RR, Borra E, Guidotti GG (2005) Cell size reduction induced by inhibition of the mTOR/S6 K-signaling pathway protects Jurkat cells from apoptosis. Cell Death Differ 12(10):1344–1357
19. Zhao Y, Wieman HL, Jacobs SR, Rathmell JC (2008) Mechanisms and methods in glucose metabolism and cell death. Methods Enzymol 442:439–457
20. Ashcroft SJ, Weerasinghe LC, Bassett JM, Randle PJ (1972) The pentose cycle and insulin release in mouse pancreatic islets. Biochem J 126(3):525–532
21. Zhao W, Zhang T, Qu B, Wu X, Zhu X, Meng F, Gu Y, Shu Y, Shen Y, Sun Y, Xu Q (2011) Sorafenib induces apoptosis in HL60 cells by inhibiting Src kinase-mediated STAT3 phosphorylation. Anticancer Drugs 22(1):79–88
22. Will Y, Dykens JA, Nadanaciva S, Hirakawa B, Jamieson J, Marroquin LD, Hynes J, Patyna S, Jessen BA (2008) Effect of the multitargeted tyrosine kinase inhibitors imatinib, dasatinib,

sunitinib, and sorafenib on mitochondrial function in isolated rat heart mitochondria and H9c2 cells. Toxicol Sci 106(1):153–161
23. Coriat R, Nicco C, Chereau C, Mir O, Alexandre J, Ropert S, Weill B, Chaussade S, Goldwasser F, Batteux F (2012) Sorafenib-induced hepatocellular carcinoma cell death depends on reactive oxygen species production in vitro and in vivo. Mol Cancer Ther 11(10):2284–2293
24. Valabrega G, Capellero S, Cavalloni G, Zaccarello G, Petrelli A, Migliardi G, Milani A, Peraldo-Neia C, Gammaitoni L, Sapino A, Pecchioni C, Moggio A, Giordano S, Aglietta M, Montemurro F (2011) HER2-positive breast cancer cells resistant to trastuzumab and lapatinib lose reliance upon HER2 and are sensitive to the multitargeted kinase inhibitor sorafenib. Breast Cancer Res Treat 130(1):29–40
25. Heravi M, Tomic N, Liang L, Devic S, Holmes J, Deblois F, Radzioch D, Muanza T (2012) Sorafenib in combination with ionizing radiation has a greater anti-tumour activity in a breast cancer model. Anticancer Drugs 23(5):525–533
26. Tran MA, Smith CD, Kester M, Robertson GP (2008) Combining nanoliposomal ceramide with sorafenib synergistically inhibits melanoma and breast cancer cell survival to decrease tumor development. Clin Cancer Res 14(11):3571–3581
27. Wilhelm SM, Adnane L, Newell P, Villanueva A, Llovet JM, Lynch M (2008) Preclinical overview of sorafenib, a multikinase inhibitor that targets both Raf and VEGF and PDGF receptor tyrosine kinase signaling. Mol Cancer Ther 7(10):3129–3140
28. O'Reilly KE, Rojo F, She QB, Solit D, Mills GB, Smith D, Lane H, Hofmann F, Hicklin DJ, Ludwig DL, Baselga J, Rosen N (2006) mTOR inhibition induces upstream receptor tyrosine kinase signaling and activates Akt. Cancer Res 66(3):1500–1508
29. Meric-Bernstam F, Akcakanat A, Chen H, Do KA, Sangai T, Adkins F, Gonzalez-Angulo AM, Rashid A, Crosby K, Dong M, Phan AT, Wolff RA, Gupta S, Mills GB, Yao J (2012) PIK3CA/PTEN mutations and Akt activation as markers of sensitivity to allosteric mTOR inhibitors. Clin Cancer Res 18(6):1777–1789
30. Rahmani M, Davis EM, Crabtree TR, Habibi JR, Nguyen TK, Dent P, Grant S (2007) The kinase inhibitor sorafenib induces cell death through a process involving induction of endoplasmic reticulum stress. Mol Cell Biol 27(15):5499–5513
31. Sanchez-Hernandez I, Baquero P, Calleros L, Chiloeches A (2012) Dual inhibition of (V600E)BRAF and the PI3K/AKT/mTOR pathway cooperates to induce apoptosis in melanoma cells through a MEK-independent mechanism. Cancer Lett 314(2):244–255
32. Ulivi P, Arienti C, Amadori D, Fabbri F, Carloni S, Tesei A, Vannini I, Silvestrini R, Zoli W (2009) Role of RAF/MEK/ERK pathway, p-STAT-3 and Mcl-1 in sorafenib activity in human pancreatic cancer cell lines. J Cell Physiol 220(1):214–221
33. Llobet D, Eritja N, Yeramian A, Pallares J, Sorolla A, Domingo M, Santacana M, Gonzalez-Tallada FJ, Matias-Guiu X, Dolcet X (2010) The multikinase inhibitor Sorafenib induces apoptosis and sensitises endometrial cancer cells to TRAIL by different mechanisms. Eur J Cancer 46(4):836–850
34. Cervello M, Bachvarov D, Lampiasi N, Cusimano A, Azzolina A, McCubrey JA, Montalto G (2012) Molecular mechanisms of sorafenib action in liver cancer cells. Cell Cycle 11(15):2843–2855
35. Cardaci S, Filomeni G, Ciriolo MR (2012) Redox implications of AMPK-mediated signal transduction beyond energetic clues. J Cell Sci 125(Pt 9):2115–2125
36. Marsin AS, Bertrand L, Rider MH, Deprez J, Beauloye C, Vincent MF, Van den Berghe G, Carling D, Hue L (2000) Phosphorylation and activation of heart PFK-2 by AMPK has a role in the stimulation of glycolysis during ischaemia. Curr Biol 10(20):1247–1255
37. Almeida A, Moncada S, Bolanos JP (2004) Nitric oxide switches on glycolysis through the AMP protein kinase and 6-phosphofructo-2-kinase pathway. Nat Cell Biol 6(1):45–51
38. Hao WS, Chang CPB, Tsao CC, Xu J (2010) Oligomycin-induced bioenergetic adaptation in cancer cells with heterogeneous bioenergetic organization. J Biol Chem 285(17):12647–12654
39. Wu SB, Wei YH (2012) AMPK-mediated increase of glycolysis as an adaptive response to oxidative stress in human cells: implication of the cell survival in mitochondrial diseases. Biochim Biophys Acta 1822(2):233–247
40. Riganti C, Gazzano E, Polimeni M, Costamagna C, Bosia A, Ghigo D (2004) Diphenyleneiodonium inhibits the cell redox metabolism and induces oxidative stress. J Biol Chem 279(46):47726–47731
41. Duvel K, Yecies JL, Menon S, Raman P, Lipovsky AI, Souza AL, Triantafellow E, Ma Q, Gorski R, Cleaver S, Vander Heiden MG, MacKeigan JP, Finan PM, Clish CB, Murphy LO, Manning BD (2010) Activation of a metabolic gene regulatory network downstream of mTOR complex 1. Mol Cell 39(2):171–183
42. Shaw RJ (2006) Glucose metabolism and cancer. Curr Opin Cell Biol 18(6):598–608
43. Shen YC, Ou DL, Hsu C, Lin KL, Chang CY, Lin CY, Liu SH, Cheng AL (2013) Activating oxidative phosphorylation by a pyruvate dehydrogenase kinase inhibitor overcomes sorafenib resistance of hepatocellular carcinoma. Br J Cancer 108(1):72–81